Revisiting the mechanisms involved in rubber deformation using experimental thermomechanics

Jean-Benoit Le Cam, José Ricardo Samaca Martinez, Xavier Balandraud, Evelyne Toussaint, Julien Caillard

Revisiting the mechanisms involved in rubber deformation using experimental thermomechanics

J.-B. Le Cam
Institut de Physique de Rennes, UMR 6251, Université De Rennes 1, Rennes, France

J.R. Samaca Martinez, X. Balandraud, E. Toussaint & J. Caillard
Clermont Université, Institut Français de Mécanique Avancée, Université Blaise Pascal, Institut Pascal, CNRS, UMR 6602, Clermont-Ferrand, France
MICHELIN, CERL Ladoux, Clermont-Ferrand, France

ABSTRACT: Most of phenomena involved in deformation of rubber depend on temperature and have distinguishable thermal and calorimetric signatures. However, since the pioneer investigations being those conducted by Gough and Joule, studies were dedicated more to mechanical response, and the thermal aspects of the deformation of rubber were not really explored experimentally. Revisiting the rubber deformation using experimental thermomechanics should offer therefore new perspectives to better understand damage and deformation mechanisms. In the present study, temperature variations are measured during the mechanical tests by means of infrared thermography. The heat sources produced or absorbed by the material due to deformation processes are deduced from the temperature variations by using the heat diffusion equation. The calorimetric signatures of the most important effects in rubber deformation have been characterized. The results bring information of importance for the understanding and the modeling of physical phenomena involved in the rubber deformation.

1 INTRODUCTION

The first studies dealing with thermomechanical properties of rubber date from the end of the 19th century, the pioneer investigations being those conducted by Gough (1805) and Joule (1857). They showed that rubber behaves mainly as an entropic elastic material, for which the retractive force is purely determined by changes in entropy and the internal energy does not change with deformation at all (Holzapfel 2000). Subsequently, studies were dedicated more to the mechanical response, and the thermal aspects of the deformation of rubber were not really explored experimentally. The first studies investigating the mechanical properties of rubber date from the beginning of the 20th century. A major result was the observation by Bouasse and Carrière (1903) of stress softening during the first mechanical cycles. This phenomenon was studied more precisely by Holt (1931) and Mullins (1948) and was then referred to as the "Mullins effect". Since these first studies, numerous other physical phenomena involved in the deformation of rubber have been highlighted, among them viscosity induced by fillers and strain-induced crystallization. Nevertheless, these phenomena are still not clearly understood, and purely mechanical studies have reached their limits in this field.

Most of these phenomena depend on temperature and have distinguishable thermal and calorimetric signatures. This is the reason why a thermomechanical analysis of rubber deformation should improve our knowledge of the mechanisms involved in rubber deformation, including entropic elasticity, reinforcement by fillers, strain-induced crystallization and stress softening. Among the possibilities available to measure temperature variations during material deformation, infrared thermography appears to be a more and more interesting approach. This technique has been widely applied to metals, polymers and composite materials (see for instance (Chrysochoos & Louche 2001) and (Berthel et al. 2007)), but rarely to elastomeric materials (Trabelsi et al. 2003; Pottier et al. 2009; Toussaint et al. 2012; Samaca Martinez et al. 2013a, 2013b). This is mainly due to difficulties in extending the measurement to the large deformations undergone by rubber (Le Cam et al. 2015).

The present paper aims first at presenting how infrared thermography and heat source calculation can be carried out in the case of the large deformations undergone by rubbers. Second, the paper deals with the thermomechanical analysis of the physical phenomena involved in rubber deformation. In order to decouple the various phenomena, several chemical compositions of rubber were used.

One of the main issues is therefore to link the physical phenomena, which occur at the microscopic scale, to the corresponding calorimetric variation measured at the macroscopic scale.

2 HEAT SOURCE CALCULATION FROM THE TEMPERATURE MEASUREMENT

The heat sources produced or absorbed by the material itself were studied within the framework of the thermodynamics of irreversible processes. In this paper, 'heat source' is used in this paper to designate the heat power density (in W/m^3) that is produced or absorbed by the material itself. The temperature fields were measured at the surface of a flat specimen using an Infrared (IR) camera. As the tests performed were assumed to be homogeneous in terms of strain and stress, and as rubbers have a very low thermal diffusivity, the temperature fields were nearly homogeneous. Therefore the 3D heat diffusion equation (1) can be reduced to a "0D" formulation as shown in (Samaca Martinez et al. 2013b, 2013c). Assuming that the heat exchanges are proportional to the temperature difference with the outside environment, the heat diffusion equation in the Lagrangian description can be written:

$$\rho C_{E,Vk}\left(\dot{\theta}+\frac{\theta}{\tau}\right)=S_h \tag{1}$$

with

$$S_h = d_1 + S_{TMC} \tag{2}$$

where:

- S_h is the heat source produced or absorbed by the material due to stretching;
- S_{TMC} is the heat source due to thermomechanical couplings. It contains the thermoelastic coupling term, mainly composed of so-called entropic coupling. It will be demonstrated in the sequel that strain-induced crystallization also contributes to S_{TMC};
- d_1 is the mechanical dissipation (always positive). It is related to any irreversible mechanical phenomenon, such as viscosity for example;
- ρ and $C_{E,Vk}$ are the density and specific heat at constant strain E and internal state variables V_k, respectively.
- θ is the temperature variation from the initial temperature (here considered in the unstretched state at the beginning of the test).
- τ □ is a characteristic time that accounts for the heat exchange with the outside environment. In practice, it can be experimentally determined by identification from a natural return to ambient temperature. This is done for different values of stretch ratio λ, which is defined as the ratio between the current and initial lengths in the considered direction. For the present experiments, the characteristic time τ was measured as an affine function of the stretch ratio λ.

Lastly, the heat source S_h is divided by the product $\rho C_{E,Vk}$, leading to a quantity s in °C/s:

$$S=\frac{S_h}{\rho C_{E,Vk}}=\dot{\theta}+\frac{\theta}{\tau} \tag{3}$$

In the following, the ratio $S/\rho C_{E,V_k}$ will be named "heat source s" for the sake of simplicity. This equation will be used to calculate the heat source s from the temperature variation θ.

3 EXPERIMENTAL SETUP

3.1 *Material and specimen geometry*

In order to highlight the calorimetric signature of the numerous phenomena involved in the deformation of rubber, i.e. entropic elasticity, strain-induced crystallization and crystallite melting, viscosity and stress softening, non-crystallizable Styrene-Butadiene Rubber (SBR) and crystallizable Natural Rubber (NR) were used, with different filler amounts. SBR was filled with two different amounts of carbon black, 5 and 50 phr (parts per hundred of rubber in weight). They are respectively denoted SBR5 and SBR50 in the following. It should be noted that fillers in SBR5 are used to improve processing; they have no significant effect on material stiffness. NR was unfilled (NR0) and filled with 50 phr of carbon black (NR50). In case of the present NR formulations, the characteristic stretch ratios at which crystallization and crystallite melting occur are denoted by λ_c and λ_m respectively, and are close to 4 and 3 for NR0 and close to 1.8 and 1.6 for NR50. The specimen geometry was a thin dumbbell-shaped specimen, whose width, height and thickness were equal to 5 mm, 10 mm and 1.4 mm respectively.

3.2 *Loading conditions*

The mechanical loading corresponded to cyclic uniaxial tensile loading. It was applied under prescribed displacement using an INSTRON 5543 testing machine. The signal shape was triangular in order to ensure a constant strain rate during loading and unloading. The loading rate and the nominal strain rate were equal to ±300 mm/min and ±0.5 s^{-1}, respectively. The test corresponded

to series of uniaxial mechanical cycles at four different maximum stretch ratios. The number of cycles was chosen in such a way that the mechanical response was stabilized. It was equal to 3 for SBR5, SBR50, NR0 and 5 for NR50. The following maximum stretch ratios were chosen for each material tested:

For the SBR5, the four maximum stretch ratios were $\lambda_1 = 2$, $\lambda_2 = 3$, $\lambda_3 = 3.5$ and $\lambda_4 = 4$;
For the SBR50, the four maximum stretch ratios were $\lambda_1 = 2$, $\lambda_2 = 3$, $\lambda_3 = 4$ and $\lambda_4 = 4.5$;
For the NR0, the four maximum stretch ratios were $\lambda_1 = 2$, $\lambda_2 = 5$, $\lambda_3 = 6$ and $\lambda_4 = 7.5$;
For the NR50, the four maximum stretch ratios were $\lambda_1 = 1.4$, $\lambda_2 = 2$, $\lambda_3 = 4$ and $\lambda_4 = 6$.

The λ_i were chosen different from one formulation to another. First, this is due to the fact that the stretches at failure were different (4.2 for SBR5 and 4.8 for SBR50, 7.9 for NR0 and 6.3 for NR50). Second, in NR0 and NR50, one stretch ratio is chosen inferior to that at which crystallization begins (about 4 for NR0 and about 1.6 for NR50).

3.3 *Full temperature field measurement*

Temperature field measurements were performed using a Cedip Jade III-MWIR infrared camera, which features a local plane array of 320 × 240 pixels and detectors with a wavelength range of 3.5–5 µm. Integration time was equal to 1500 µs. The acquisition frequency f_a was 147 Hz. The thermal resolution, namely the noise-equivalent temperature difference, was equal to 0.02°C for a temperature range of 5–40 °C. The calibration of the camera detectors was performed with a black body using a Non-Uniformity Correction (NUC) procedure. During the measurements, the external heat sources were reduced by using a black box surrounding the specimen, featuring a small window for the IR camera to be able to observe the gauge zone of the specimen. A suitable movement compensation technique was used to track the small zone at the centre of specimen surface during the test (see for instance (Pottier et al. 2009)).

4 RESULTS AND ANALYSIS

4.1 *Mechanical and thermal responses*

The mechanical response of NR0, NR50, SBR5 and SBR50 is given in Figures 1(a), (b), (c) and (d), respectively. These figures present the nominal stress, defined as the force per initial surface ratio, versus the stretch ratio. Several comments can be made:

1. NR0 and SBR5 did not exhibit significant stress softening, *i.e.* mechanical cycles had no effect on the mechanical response (see Fig. 1(a) for NR0 and 1(c) for SBR5). This is classically observed in unfilled or barely-filled rubbers;
2. No significant permanent strain was observed in NR0;
3. In SBR5, no significant hysteresis loop was observed, but the residual strain reached 15%. This can be explained by the presence of fillers, even in small amounts;
4. In NR0, no hysteresis loop was observed when the maximum stretch ratio did not significantly exceed that at which crystallization starts (about 4 for this formulation); for higher maximum stretch ratios, a significant hysteresis loop was observed. It is now clearly established that this phenomenon is due to the difference in the kinetics of crystallization and crystallite melting (Trabelsi et al. 2003; Le Cam & Toussaint, 2008);
5. When fillers were added to the compounds, a hysteresis loop was observed in SBR50 (see Fig. 1(d)). Moreover, the permanent strain increased. The mechanical response of NR50 also exhibited a larger hysteresis loop (occurring for stretch ratios lower than for NR0) and larger residual strains.

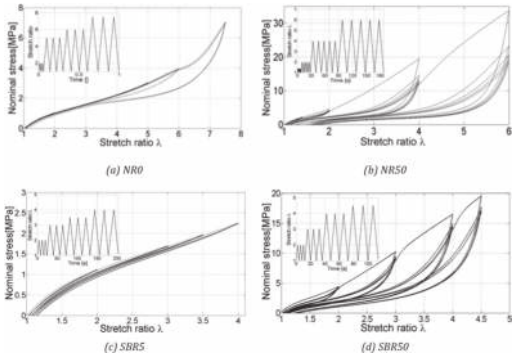

Figure 1. Loading conditions and mechanical responses obtained for the four compounds during cyclic uniaxial tensile tests.

The thermal responses obtained during the tests are precisely detailed and discussed in (Le Cam et al. 2015). The conclusion of this study is that temperature variation is influenced by heat exchanges, which complicates the analysis, and it is not possible to decouple the effects of entropic elasticity, viscosity and stress softening, *i.e.* to decouple the effects of thermomechanical coupling and mechanical dissipation. This is the reason why heat source is more suitable than temperature to analyze the thermomechanical response of rubber.

4.2 *Calorimetric responses*

Figure 2 presents the calorimetric response obtained for each compound during cyclic tests. These figures, which present the heat sources in °C/s versus time, allow us to present successively the different phenomena that affect the calorimetric responses. They are more precisely investigated in the following sections.

Several results are highlighted by these figures:

1. For all the compounds, an increase in the stretch ratio induces an increase in the heat source. This is a consequence of the entropic elasticity of rubber. This is more precisely investigated with SBR5 in the next section, "Heat sources due to entropic elasticity". It can be noted that, at the lowest stretch ratios, a thermoelastic inversion was observed. This is not addressed in this paper, but the reader can refer to (Pottier et al. 2009) for further information on the effect of this phenomenon on the heat sources. In NR, when the stretch ratio at which crystallization begins was exceeded (about 4.2 for NR0 and 1.6 for NR50), a high increase in the heat source was observed. This is investigated in the "Heat sources due to strain-induced crystallization and crystallite melting" section.
2. In filled NR, the stabilized heat source is close to the maximum heat source obtained in unfilled NR at a given maximum stretch ratio, which was not true for SBR. Indeed, at $\lambda = 4$, the heat source in SBR50 was approximately 4 times that in SBR5. This is addressed in detail in the section "Heat sources due to filler effect".

In NR0 and SBR5, the calorimetric response did not depend on the number of cycles at a given maximum stretch. When fillers were added to the compounds, the first mechanical cycle at a given maximum stretch ratio led to a higher maximum heat source, but the same minimum heat source as for the other cycles. Moreover, the stabilization of the calorimetric response occurred at the third cycle in SBR50 and at the fifth cycle in NR50. This has a strong similarity with the stress softening phenomenon, and is more precisely investigated in the section "The calorimetric signature of the Mullins effect".

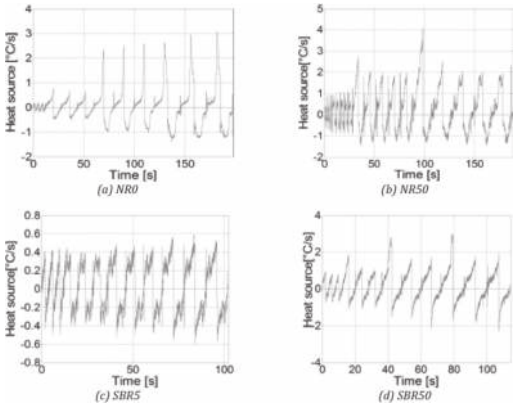

Figure 2. Heat source evolution obtained for the four compounds during cyclic uniaxial tensile tests.

4.3 *Heat sources due to entropic elasticity*

In order to discuss the calorimetric response due to entropic elasticity only, SBR5 was chosen. Indeed, SBR5 did not exhibit any viscosity or stress softening and was not subjected to strain-induced crystallization. It can be noted that NR0 could also have been chosen for this discussion, but for maximum stretch ratios inferior to λ_c. Figure 3 presents the heat source versus the stretch ratio obtained for the first (stabilized) cycle for each maximum stretch ratio applied: 2, 3, 3.5 and 4 in Figs. 3(a), (b), (c) and (d), respectively. It can be noted that the residual strain induced buckling and that the surface to be observed did not remain flat in that case. Consequently, the temperature measurement is incorrect close to zero strain. This is the reason why in these figures and the following ones there is a grey zone indicating the range of stretch ratios for which the heat source assessments were not valid.

As shown in these figures, heat source variations during loading and unloading were the same in absolute value whatever the maximum stretch ratio applied (in these figures, the light continuous lines correspond to the absolute value of the heat source during unloading). This means that no dissipation occurs during the mechanical cycles, which is in good agreement with the fact that no significant mechanical hysteresis was observed.

4.4 *Heat sources due to strain-induced crystallization and crystallite melting*

The effects of strain-induced crystallization and crystallite melting were studied with NR0. This compound exhibited neither a hysteresis loop due to viscosity nor stress softening. Therefore the singularities in the calorimetric response can only be due to strain-induced crystallization and crystallite melting. As previously explained, four series of three uniaxial mechanical cycles were applied with four increasing maximum stretch ratios, series #1 with $\lambda_1 = 2$, series #2 with $\lambda_2 = 5$, series #3 with $\lambda_3 = 6$ and series #4 with $\lambda_4 = 7.5$.

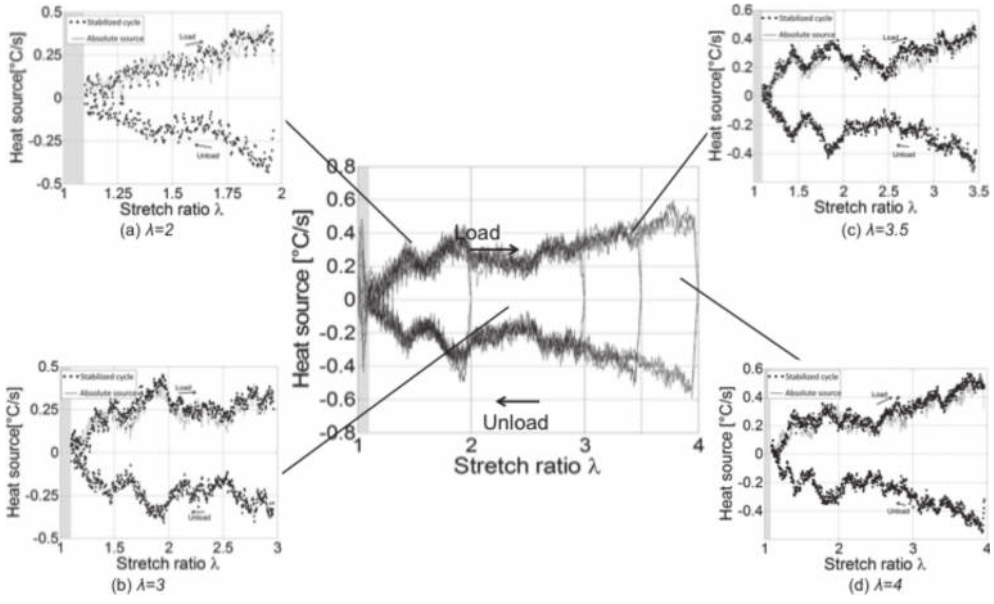

Figure 3. Heat source versus stretch ratio obtained for SBR5. The light continuous lines correspond to the absolute value of the heat source during unloading.

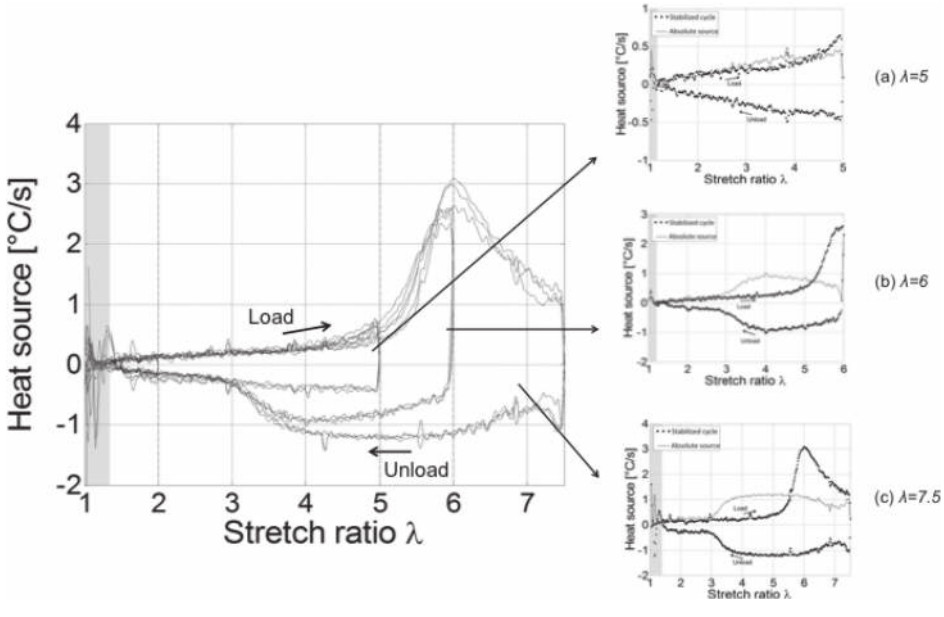

Figure 4. Heat source versus stretch ratio obtained for NR0. The light continuous lines correspond to the absolute value of the heat source during unloading.

Figure 4 (left) presents the heat source versus the stretch ratio during the test. The first series of cycles, for stretch ratios superior to λ_c, are presented in the diagrams on the right-hand side. When the maximum stretch ratio was inferior to λ_c, the heat source evolutions for loading and unloading were symmetrical. This means that no mechanical dissipation occurred.

For series with a maximum stretch ratio equal to 5, the heat source evolutions were not symmetrical. During loading, the heat source evolves in a quasi-linear manner until reaching a stretch ratio close to 4. The only change in the microstructure in NR is the strain-induced crystallization. It starts at a stretch ratio of approximately 4. Consequently, the only phenomenon that changes the temperature at stretch ratio inferior to 4 is the thermoelasticity. As the heat source increased quasi-linearly during loading and decreased during unloading, the heat source evolution is mainly due to entropic thermoelasticity. Let us recall that a heat source evolution due to energetic thermoelasticity at constant strain rate does not depend on the stretch level and is negative during loading and positive during unloading. A dissymmetry was observed for higher maximum stretch ratios. This indicates that the heat sources are not caused only by entropic elasticity. Moreover, the area under the curves during loading and unloading was equal, meaning that no heat was produced due to mechanical dissipation. Consequently, the only explanation for the dissymmetry is the occurrence of crystallization during loading, and a difference in the kinetics of crystallization and crystallite melting (the latter during unloading). This is in good agreement with studies reported in the literature (Trabelsi et al. 2003). Concerning the stress-strain curve, a hysteresis loop began to form. It is associated with the crystallization/melting phenomenon, and not with mechanical dissipation. Indeed, if no crystallization occurred, no hysteresis loop was observed for the strain-stress relationship. When the maximum applied stretch ratio increased, loading-unloading dissymmetry increased. From a mechanical point of view, the area of the hysteresis loop also increased. Once again, as the heat produced was equal to the heat absorbed, no mechanical dissipation was detected, while a mechanical hysteresis loop was observed. It should be noted that crystallization induces a strong increase in the heat source, and from stretch ratios equal to 6 during the loading phase, instead of increasing continuously, the heat source decreased. This means that heat continues to be produced (it remains positive), but at a lower rate. This phenomenon could be due to several causes:

1. the fact that this level of stretch ratio would tend to approach crystallinity saturation if any;
2. an increase in the contribution of internal energy;

a less exothermal crystallization process. It should be noted that the hysteresis area in terms of the strain-stress relationship is higher than previously, again with no mechanical dissipation detected.

4.5 *Heat sources due to filler effect*

When fillers are added to the compounds, stress softening is observed. This phenomenon is investigated in the next section. In order to focus only on the effects of fillers on the stationary calorimetric response, the stabilized cycles obtained for SBR50 and NR50 are considered. They are presented in Figures 5 and 6, respectively. For NR50, only the last two maximum stretch ratios applied are presented, due to the fact that a significant permanent set (compared to the maximum stretch ratio applied) was observed for the first two maximum stretch ratios applied. This permanent set induced buckling which disturbed the temperature measurement. Consequently, we have not calculated heat sources for these cycles. As in the previous figure, the global response in terms of the heat sources versus the stretch ratio during the test is indicated, as well as the stabilized calorimetric response at given maximum stretch ratios.

Heat source evolutions obtained with SBR50 and NR50 exhibit load-unload dissymmetry. This appears clearly by comparing the heat source obtained during loading with its absolute value during unloading. As SBR is not subjected to strain-induced crystallization and crystallite melting, this shows that mechanical dissipation is produced, even if the calorimetric response is stabilized. This mechanical dissipation is due to viscosity, which is induced (in NR) or amplified (in SBR) by adding fillers. In NR50, the same phenomenon was observed. Moreover, in NR50, adding fillers did not significantly increase the heat source produced. As expected, the increase (decrease) in the heat source produced (absorbed) during loading (unloading) due to the onset of crystallization (melting had finished) occurred at a lower stretch ratio than in NR0.

4.6 *The calorimetric signature of the Mullins effect*

From a mechanical point of view, a major result obtained from the mechanical tests was the observation of the decrease in rubber stiffness during the first mechanical cycles. This phenomenon is referred to as “the Mullins effect” in the literature. Up to now, this effect has mainly been investigated from a mechanical point of view, while its thermal and calorimetric signatures might also contain information of importance about it.

Figure 7 presents the heat source versus stretch ratio for series of three first cycles at four increasing maximum stretch ratios in SBR50. First, whatever the maximum stretch ratio, the heat source

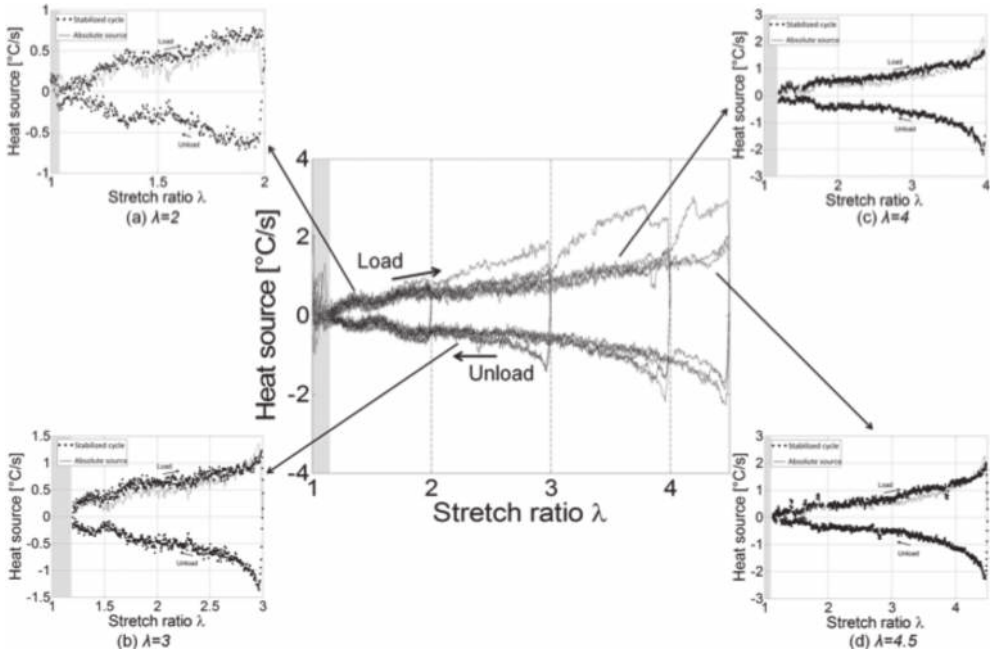

Figure 5. Heat source versus stretch ratio obtained for SBR50. The light continuous lines correspond to the absolute value of the heat source during unloading.

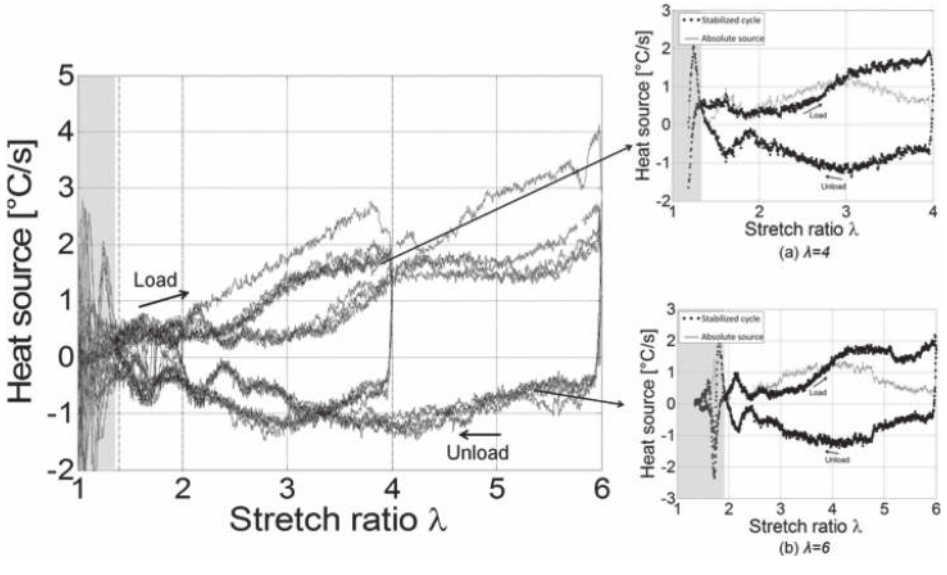

Figure 6. Heat source versus stretch ratio obtained for NR50. The light continuous lines correspond to the absolute value of the heat source during unloading.

produced is higher during the first cycle. The following cycles are stabilized. This is the first similarity with the Mullins effect. Second, a decrease in the heat source appears for stretch ratios lower or equal to the maximum stretch previously applied. When the stretch ratio exceeds the maximum stretch ratio previously applied, the calorimetric response greatly increases.

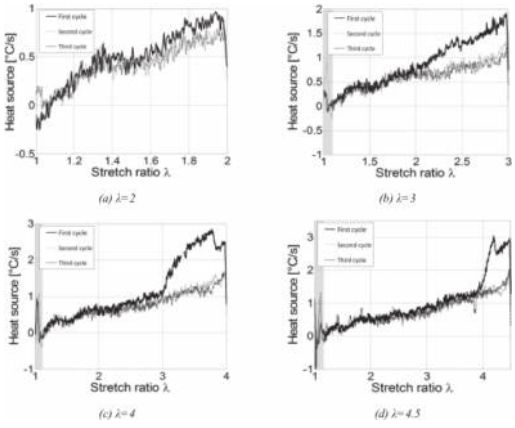

Figure 7. Heat source obtained during the loading phase for SBR50.

The loss in the heat source increases with the increasing maximum stretch ratio. Measurement of the calorimetric response allows us to deduce the mechanical dissipation induced by stress softening. It can be calculated by the difference in mechanical dissipation between the first and the stabilized cycles.

The results are more difficult to analyze in crystallizable filled natural rubber. Even though strain-induced crystallization and crystallite melting did not change this tendency, during the first loading the heat source due to crystallization was "hidden" in the total heat source (including mechanical dissipation due to damage). This is precisely detailed in (Samaca Martinez et al. 2014).

5 CONCLUSION

This study has addressed the calorimetric response associated with deformation processes in different formulations of rubbers: filled and unfilled non-crystallizable SBR and crystallizable NR. These formulations have enabled us to investigate the calorimetric signature of the main physical phenomena involved in rubber deformation: entropic elasticity, strain-induced crystallization, reinforcement by fillers and stress softening. The rubber formulations were chosen in such a way that these phenomena could be studied separately. The main results can be summarized as follows:

– Entropic elasticity leads to heat production (absorption) when the rubber is stretched (relaxed). The heat source—strain relationship is quasi-linear. Load-unload heat source curves are symmetrical.
– The kinetics and therefore the calorimetric signature of strain-induced crystallization differs from that of crystallite melting, so that no symmetry is observed in terms of heat source between loading and unloading. Nevertheless, the areas under the load-unload curves are equal, meaning that crystallization and melting occur without detectable corresponding mechanical dissipation.
– Fillers induce viscosity and therefore mechanical dissipation (positive heat source) during both loading and unloading, which increases when the maximum stretch ratio increases. In filled NR, significant heat production is observed at a lower stretch ratio than in unfilled NR, and mechanical dissipation is detected.
– Numerous similarities are observed between the mechanical and the calorimetric responses. First, the stabilization of the calorimetric response is reached at the end of the first cycle, similarly to the mechanical response. Second, the higher the maximum stretch ratio applied, the higher the heat source decrease between the first and second cycles. It should be noted that, contrary to the mechanical response, the calorimetric response enables us to detect changes in the characteristic stretch ratios at which strain-induced crystallization starts and crystallite melting is complete.

ACKNOWLEDGEMENTS

The authors would like to acknowledge the "Manufacture Française des Pneumatiques Michelin" for supporting this study.

REFERENCES

Berthel B, Wattrisse B, Chrysochoos A, Galtier A. 2007. Thermoelastic analysis of fatigue dissipation properties of steel sheets. Strain 43:273–279.

Bouasse H, Carrière Z. 1903. Courbes de traction du caoutchouc vulcanisé. Annales de la Faculté des Sciences de Toulouse 5:257–283.

Chrysochoos A. 1995. Analyse du comportement des matériaux par thermographie Infra Rouge, in: Eyrolles (Ed.), Colloque Photomécanique. pp. 203–211.

Chrysochoos A, Louche H. 2001. Thermal and dissipative effects accompanying luders band propagation. Mat Sci Eng A-struct 307:15–22.

Gough J. 1805. A description of a property of Caoutchouc or India Rubber. Porc. Lit. Phil. Soc. Manchester, 2nd series 1:288–295.

Holt WL. 1931. Behavior of rubber under repeated stresses. Journal of Industrial and Engineering Chemistry 23:1471–1475.

Holzapfel GA. 2000. Nonlinear Solid Mechanics. A Continuum Approach for Engineering. Ed. John Wiley & Sons Ltd.

Joule JP. 1857. On some thermodynamic properties of solids. Phil Mag 4th 14:227.

Le Cam JB, Toussaint E. 2008. Volume variation in stretched natural rubber: competition between cavitation and stress-induced crystallization. Macromolecules 41:7579–7583.

Le Cam JB. 2012. A review of the challenges and limitations of full-field measurements applied to large heterogeneous deformations of rubbers. Strain 48:174–188.

Le Cam JB, Samaca Martinez JR, Toussaint E, Balandraud X, Caillard J. 2015. Thermomechanical Analysis of the Singular Behavior of Rubber: Entropic Elasticity, Reinforcement by Fillers, Strain-Induced Crystallization and the Mullins Effect. Part 2: quantitative calorimetric analysis. Polymer 55:771–782.

Mullins L. 1948. Effect of stretching on the properties of rubber. Rubber Chemistry and Technology 21:281–300.

Pottier T, Moutrille MP, Le Cam JB, Balandraud X, Grédiac M. 2009. Study on the use of motion compensation techniques to determine heat sources. Application to large deformations on cracked rubber specimens. Exp Mech 49:561–574.

Samaca Martinez JR, Le Cam JB, Toussaint E, Balandraud X, Caillard J. 2013a. Mechanisms of deformation in crystallizable natural rubber. Part 1: thermal characterization. Polymer 54: 2717–2726.

Samaca Martinez JR, Le Cam JB, Toussaint E, Balandraud X, Caillard J. 2013b. Mechanisms of deformation in crystallizable natural rubber. Part 2: quantitative calorimetric analysis. Polymer 54:2727–2736.

Samaca Martinez JR, Le Cam JB, Toussaint E, Balandraud X, Caillard J. 2013c. Filler effects on the thermomechanical response of stretched rubbers. Polymer Testing 32:835–841.

Toussaint E, Balandraud X, Le Cam JB, Grédiac M. 2012. Combining displacement, strain, temperature and heat source fields to investigate the thermomechanical response of an elastomeric specimen subjected to large deformations. Polym Test 31:916–925.

Trabelsi S, Albouy PA, Rault J. 2003. Crystallization and Melting Processes in Vulcanized Stretched Natural Rubber. Macromolecules 36:7624–7639.